
An Analysis of the Arterial Input Curve for Technetium-99m-HMPAO: Quantification of rCBF Using Single-Photon Emission Computed Tomography

Alberto Pupi, Maria Teresa R. De Cristofaro, Lucia Bacciottini, Davide Antonucci, Andreas R. Formiconi, Mario Mascalchi, and Ugo Meldolesi

Sezione di Medicina Nucleare, Dipartimento di Fisiopatologia Clinica, U.O. Cardiologia, USL 10/D Firenze, and Sezione di Radiologia, Dipartimento di Fisiopatologia Clinica, Università di Firenze, Firenze, Italy

Arterial radioactivity content after the intravenous administration of HMPAO in seven human subjects was analyzed. Arterial sampling of ^{99m}Tc-HMPAO was performed on each subject over a 25-min period postinjection. The lipophilic fraction of the tracer present in the blood was rapidly extracted with octanol. An analysis of the time course of the extracted and nonextracted octanol fractions was performed in order to calculate the arterial input of the tracer available for brain extraction. HMPAO net regional brain clearances were then calculated and compared with rCBF values obtained in the same patients using ^{99m}Tc-microspheres injected into the left ventricle of the heart. HMPAO brain clearances were 0.41 ± 0.01 and 0.27 ± 0.01 ml/min/g for grey and white matter, respectively. Linear regression analysis was performed and the following result was obtained:

$$\text{Clearance (HMPAO)} = 0.07 + 0.43 \cdot \text{rCBF}$$

with a high significance ($p < 0.001$). This equation can be used for the transformation of HMPAO clearances into rCBF values. Our study demonstrates that by using HMPAO and SPECT it is possible to obtain a quantitative estimate of rCBF in humans.

J Nucl Med 1991; 32:1501-1506

Technetium-99m-d, 1-hexamethyl - propylene - amine-oxime, HMPAO (Ceretek, Amersham Ltd, Buckinghamshire, England) is a blood-brain barrier-crossing (BBB) tracer. It remains trapped in the brain, in relation to rCBF (1). Analysis and description of the kinetics of this tracer in the brain eventually led to the formulation of an algorithm that corrects for extraction limitation and backflux of HMPAO. This results in a more linear relation between rCBF and HMPAO distribution (2). Quantitative ap-

proaches have also been attempted using autoradiography and the measurement of the tracer arterial input function (3). The major limitations in assessing arterial input function were identified as the combination of the circulating radioactive tracer (diffusible) and its non-BBB crossing radioactive conversion products (non-diffusible) (4). It is quite difficult to separate the two previously mentioned fractions. If we compare the speed with which the former is transformed into the latter in the blood, and the time needed for typical analytical procedures (paper or column chromatography), then the reason for this difficulty becomes obvious. Andersen et al. (4) applied the rapid octanol extraction technique—first proposed for N-isopropyl-p-[¹²³I]iodoamphetamine (5)—to study and measure the arterial concentration of the lipophilic fraction in humans. This technique was not subsequently used to quantify rCBF with HMPAO. Matsuda et al. (6) reported a quantitative approach using a model which took both brain and blood tracer kinetics into account. Kinetic parameters were obtained with a multiparametric fitting based on multiple fast SPECT acquisitions as well as arterial radioactivity sampling.

The present work analyzes the arterial radioactivity content in humans after intravenous injection of HMPAO. It focuses on the separation of different tracer fractions, using the octanol extraction technique. The SPECT measurement of brain activity and the data from the analysis of the previously mentioned technique enabled us to calculate the net regional brain HMPAO clearance values. The latter were then compared to the rCBF values obtained in the same subjects using ^{99m}Tc-microspheres. Our results demonstrate that it is possible to obtain a quantitative estimate of rCBF using HMPAO and single-photon emission computed tomography (SPECT).

MATERIALS AND METHODS

Patients and Protocol

Seven right-handed male patients (aged between 40 and 70 yr), affected by cardiovascular disease (without overt cardiac failure)

Received Aug. 28, 1990; revision accepted Apr. 23, 1991
For reprints contact: Alberto Pupi, MD, Sezione di Medicina Nucleare, Dipartimento di Fisiopatologia Clinica, Viale Morgagni 85, 50134 Firenze, Italy.

and needing left heart catheterization with left ventriculography and coronary angiography, were recruited for this study. Descriptive data and clinical characteristics of the patients are reported in Table 1. All patients gave their informed consent.

Patients showed no previous history of neurologic disease and no neurologic symptoms were found on examination. A magnetic resonance imaging (MRI) study (Philips, Gyroscan, 0.5 T) also was performed in five of them. Of these, one patient refused MRI on account of claustrophobia. MRI, however, demonstrated no tissue alteration in the other four patients. The sulcal and ventricular spaces were within the normal range, considering the age range of the patients. SPECT with HMPAO was performed first; two days later brain SPECT was performed following the injection of microspheres into the left ventricle during cardiac catheterization.

Tracers

Human serum albumin microspheres, particle size 15 μm , (Spherotec-S, Sorin, Saluggia, Italy) were labeled with $^{99\text{m}}\text{Tc}$, (2 GBq in 5 ml of saline). They were then sonicated (USR05, Julabo Labortechnik, GMBH) until the moment of injection.

The $^{99\text{m}}\text{Tc}$ -HMPAO complex was obtained by adding 3 ml of fresh eluent of $^{99\text{m}}\text{Tc}$ -pertechnetate solution (2 GBq) to 0.5 mg of freeze-dried HMPAO in commercially supplied vials. Immediately before the injection of the tracer, the radiochemical purity (RCP) of HMPAO was assessed using paper chromatography, as described elsewhere (7), and was found to be $97.2\% \pm 0.74\%$ (mean \pm s.e.m.).

HMPAO Study

A No. 20-gauge catheter (RA-04020-E, Arrow, Reading, PA) was inserted into the radial artery of the left arm under local anesthesia (Lidocaine 2%). The catheter was directly connected to the tube (0.03 in. in inner diameter, Elkay, U.K.) of a peristaltic pump (Minipuls 2, Gilson, France). One empty pre-weighed vial was used to collect a 20-sec blood sample so as to calculate the pump outlet in mg/min. Blood density was taken as 1.05 g/ml (8). The pump was set at its maximum speed for a mean flow of 1.4 ml/min. The inlet-outlet transit time of the withdrawal tubing

system (pump included) was 7 sec. A venous cannula was inserted into an antecubital vein of the right arm. The HMPAO dose (1 GBq in 1.5 ml) was pre-loaded into a tube connected to this cannula and then rapidly flushed with a 20-ml saline bolus. On injection, continuous arterial sampling was started and the withdrawal flow was regulated by the peristaltic pump. Sampling lasted 25 min and consisted of collecting consecutive 5-sec samples for the first 3 min and then a 5-sec sample each minute. The arterial blood samples were collected by placing the distal end of the peristaltic pump tube directly inside the vials containing 1 ml of octanol (E. Merck, D-6100 Darmstadt, Germany). Each vial was mechanically shaken on collection. When arterial sampling was completed, the vials were centrifuged (1500 g for 10 min) to separate the two phases, and 500 μl of the octanol phase were transferred into an empty vial. This vial and the one containing the remains of the biphasic system were counted in a well counter (1197, Gamma Counting System, Searle Analytic Inc.). The octanol-extracted radioactivity (OER) and the total radioactivity (TR) were calculated. The difference between TR and OER was calculated as the nonextracted radioactivity (NOER). HMPAO SPECT followed the arterial sampling (i.e., 35 min after the injection of the tracer).

Analysis of the HMPAO Blood Samples

The time courses of TR, OER, and NOER are shown in Figure 1. They are determined by the following: (1) the input function of HMPAO in the blood stream, (2) the blood-tissue exchanges in the capillary spaces, and (3) the conversion of the radioactive diffusible fraction (DR) into the non-diffusible one (NDR). DR cannot be expected to maintain a constant concentration in the blood since, on the one hand, it converts to NDR and, on the other, it passes into the tissue where it is trapped in part. Therefore, if DR alone were extracted in the octanol phase, the OER curve would progressively decrease until it reached the sensitivity limit of the counting system (well counter). On the contrary, we found that the final part of the OER curve shows a plateau phase which starts at a plateau time (Pt) and moves forward (Fig. 1). In our opinion, this could be explained by having:

1. OER represents not only DR, but also a fraction of NDR extracted by octanol (NDR_F).
2. OER contains solely NDR_F , for $t > \text{Pt}$:

To try and quantify DR, we propose the following assumptions:

1. NDR_F is proportional to NOER in relation to a factor K.
2. K is constant during the entire arterial sampling.

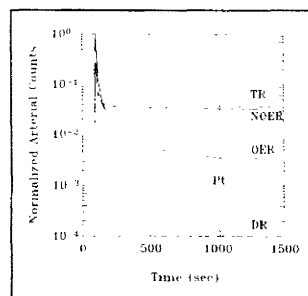
TABLE 1

Descriptive Data and Clinical Characteristics of Patients

Patient no.	Sex	Age	Heart disease
1	M	56	Anterior MI, LV aneurysm, LV dysfunction
2	M	66	Anterior and inferior MI, LV aneurysm, postinfarction angina
3	M	40	Effort angina with severe perfusion defect in ^{201}Tl MS
4	M	61	Infero-lateral MI, postinfarction angina
5	M	54	Silent inferior MI, postinfarction silent ischemia
6	M	51	Non-Q anteroseptal MI, postinfarction silent ischemia
7	M	70	Non-Q anteroseptal MI, postinfarction silent ischemia

LV = left ventricle; MI = myocardial infarct; and MS = myocardial scintigraphy

FIGURE 1. Time course of the various fractions of radioactivity in the arterial blood in a representative case (Patient 6). TR = total radioactivity; NOER = nonoctanol extracted radioactivity; OER = octanol-extracted radioactivity; DR = diffusible radioactivity. Data are normalized to the peak of TR. The dotted line delineates the plateau time (Pt).



The proportionality factor K can be estimated as the mean of the OER/NOER ratios of all the samples with $t > Pt$, since for such time

$$\text{OER}(t)/\text{NOER}(t) = \text{NDR}_E(t)/\text{NOER}(t) = K \quad t > Pt.$$

Thus, DR is to be calculated as:

$$\text{DR}(t) = \text{OER}(t) - [\text{NOER}(t) \cdot K].$$

Figure 1 also reports the time course of DR. This curve approaches zero a few minutes after the injection of HMPAO. In this way, it allows the end time of the experiment (ETE) to be defined. ETE is defined as the time in which the DR(t) integral reaches 99% of its 25th min value (Fig. 2). The DR(t) integral nearly reaches a constant value a few minutes after the injection (Fig. 2), while the integrals of TR and, to a lesser extent, OER continue to increase. The stable final value of the DR(t) integral, denoted by Q_{HMPAO} , represents the total radioactivity available for extraction across the BBB. In the experiment, Q_{HMPAO} was decay-corrected to the time of middle HMPAO SPECT acquisition.

Microsphere Study

Under sterile conditions a No. 8F sheath was positioned in the right femoral artery using percutaneous puncture. A No. 7 pigtail catheter was inserted and advanced to the apex of the left ventricle. A 60-cm tube was attached to the side arm of the sheath to collect blood from the femoral artery. Arterial withdrawal was controlled by a peristaltic pump (Minipuls 2, Gilson, France) equipped with a catheter with an inner diameter of 0.11 inches (Elkay, U.K.). One empty pre-weighed vial was used to collect a blood sample for 20 sec, so as to calculate the pump outlet in mg/min. Blood density was assumed to be 1.05 g/ml (8). The pump was set at its maximum speed which corresponded to a mean flow of 12 ml/min.

Two million microspheres, labeled with 1 GBq of ^{99m}Tc , were injected into the left ventricle with a slow 20-ml saline bolus. Blood was collected in separate heparinized vials (one every 20 sec) and the collection continued until 4 min after the injection. Left ventriculography and coronary angiography were performed once arterial sampling had been completed. Blood samples were centrifuged (1500 g for 15 min) and the supernatant was separated in order to discard the radioactivity not bound to microspheres. The remainder was counted in a well counter (1197 Gamma Counting System, Searle Analytic Inc.). The radioactivity content (Q_{MI}) was integrated until the end of the arterial sampling, but it was virtually non-existent at the end of the 2nd min. Then Q_{MI} was decay-corrected to the time of middle microsphere SPECT acquisition.

Following radiologic examination, the patients were referred to the Nuclear Medicine Unit and brain SPECT was performed. The latter was begun 45 min after microsphere injection.

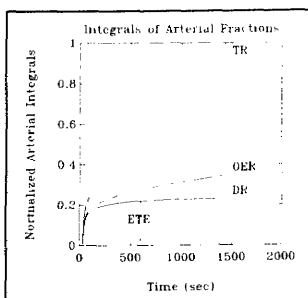


FIGURE 2. The integrated arterial concentration of the various fractions of radioactivity in a representative case (Patient 6). Data are normalized to the 25th min value of the integral of TR. The vertical dotted line shows the end time of the experiment (ETE).

SPECT Study

Both HMPAO and microsphere brain SPECT were performed using a dual head rotating camera (Rotacamera, Siemens Gammasonics, Des Plaines, IL), equipped with ultra high-resolution collimators. Linear sampling of the projections measured 4.5 mm on both planes. Ninety projections were acquired with each camera head during a 360° rotation. The projection time lasted 25 sec for the HMPAO SPECT and 15 sec for the microsphere SPECT, so as to balance the number of counts acquired. Reconstruction was performed using data from both camera heads, using the iterative least squares algorithm, which compensates for collimator spatial response and affords a FWHM of 8 mm (9). Ten iterations resulted in optimum image quality.

Both SPECT studies were orientated (10) on the fronto-occipital line (11) and were anatomically matched. Two slices, each 9 mm thick, were selected at the supraventricular and midthalamic levels (Fig. 3). A superimposition algorithm (12) was used to find the spatial correspondence between microsphere and HMPAO images. For each case studied, 21 anatomical ROIs, delineating various cortical and subcortical structures, were drawn manually by an experienced physician (MTRDC).

A cross-calibration factor (CCF), which was specific for each ROI, was calculated as described elsewhere (13), using an anatomical midthalamic brain phantom (for the midthalamic level) and a cylindrical phantom, 15 cm in diameter, (for the supraventricular level). CCF enabled us to express ROI activity concentrations (C_{ISPECT}) in counts/ml with the same efficiency as the well counter used to count blood samples.

Data Analysis

In the same way, net regional brain HMPAO clearance (rC_{HMPAO}) and $r\text{CBF}$ values were calculated as the ratio:

$$(C_{\text{ISPECT}} \cdot Fa)/Qa,$$

where C_{ISPECT} , Qa and Fa are the tissue radioactivity concentration, the arterial input and withdrawal rate of the pump (ml/min), for HMPAO and microspheres, respectively. The HMPAO retained fractions (RF) were calculated for each ROI as the ratio:

$$rC_{\text{HMPAO}}/r\text{CBF}.$$

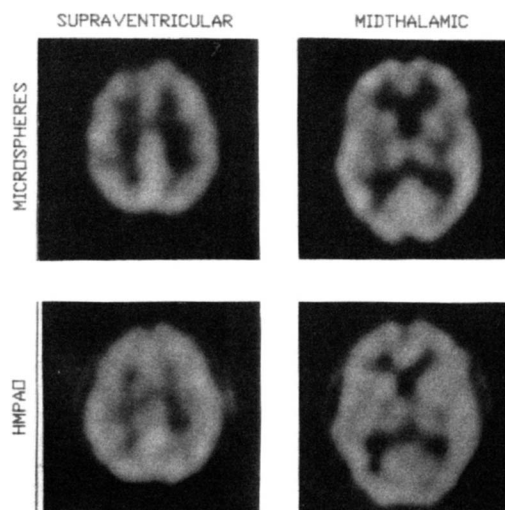


FIGURE 3. Nine-millimeter thick anatomically matched microspheres and HMPAO SPECT slices of one case (Patient 2). The grey/white ratio is 1.55 for microspheres and 1.33 for HMPAO.

RESULTS

The K proportionality factor, determined from the analysis of the arterial curve, averaged 0.121 ± 0.013 (mean \pm s.e.m.). In other words, it can be said that, in the blood, there is 12% of lipophilic radioactivity which is non-diffusible. ETE was 635 ± 35 sec (mean \pm s.e.m.), i.e., about 10 min after the injection there is no diffusible radioactivity in the blood.

The visual inspection of microsphere and HMPAO images shows that microsphere images have a higher contrast. However, the regional distribution of the two tracers is quite similar (Fig. 3).

The rCBF and rCl_{pao} values (mean \pm s.e.m.) and the volume of the tissue samples are summarized in Table 2, which reports a selection of the brain regions examined.

The rCBF values range from 0.28 to 0.96 ml/min/g, and three-quarters of them are above 0.6 ml/min/g. The rCl_{pao} values range from 0.19 to 0.59 ml/min/g, and three-quarters of them exceed 0.33 ml/min/g. The mean RF of HMPAO for the 147 ROIs is 0.55 ± 0.10 (mean \pm s.d.).

An rCBF and rCl_{pao} plot is reported in Figure 4. The linear regression equation is:

$$rCl_{pao} = 0.07 + 0.43 \cdot rCBF.$$

The analysis of variance of the regression gives a highly significant F value ($F = 176$, $p < 0.001$).

When the regression analysis between rCBF and rCl_{pao} was done on a patient-by-patient basis, the intercept value resulted in 0.07 ± 0.02 and the angular coefficient value resulted in 0.43 ± 0.02 (mean \pm s.e.m.). The p value was always below 0.001.

DISCUSSION

The development of single-photon labeled tracers that become trapped in the brain as a function of rCBF enables SPECT to be used to quantitate brain perfusion. Given the inherent characteristics of SPECT acquisition (rotation), the method of choice used with SPECT relies on

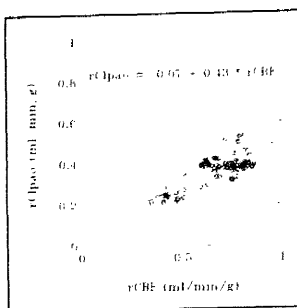


FIGURE 4. Comparison of rCBF and rCl_{pao}. The plot reports 147 points, corresponding to the 21 ROIs extracted in each of the seven patients. The continuous line represents the linear regression.

single tissue concentration measurement (i.e., autoradiographic method). To be correctly applied, this method requires an ETE to be established. For tracers with brain kinetics described by the one-compartment model (e.g., iodoantipyrine), ETE corresponds to the moment of sacrifice in animal experiments. On the other hand, for two-compartment model tracers, ETE is determined by the biologic behaviour of the tracer. In fact, it corresponds to the moment when the circulating activity no longer diffuses across the BBB and the brain retained tracer is completely entrapped.

In the case of HMPAO, the first requisite is satisfied since, 10 min after the injection, brain activity is stable for a sufficient length of time to enable SPECT acquisition (7). As to the second requisite, the blood still retains some radioactivity that cannot diffuse across the BBB (TR curve in Fig. 1). Thus, the measurement of total blood activity does not represent the arterial input function into the brain. Our results show that a minimal quantity of OER is still present until the 25th minute postinjection (p.i.). We want to emphasize that a 25% increase in the integral of OER may consequently follow from the 10th to the 25th min p.i. (Fig. 2), while the integral of DR increases only by about 1% in this same time interval.

Our hypothesis that OER contains an aliquot of NDR (NDR_E) is based on the following: after injection, the activity concentration in the brain (which can be considered a probe for the presence of DR in the blood) does not increase after the first few minutes, while OER remains significant. As regards the composition of NDR_E, the 12% value of the NDR_E/NOER ratio can, in part, be justified by the 1% partition coefficient octanol: blood of the hydrophilic forms of HMPAO (4) and by the blood: octanol volume ratio of 1:8.5 used in this study. In fact, Andersen et al. (4) demonstrated that the arterial octanol extracted radioactivity, corrected for the partition coefficients of the other radioactive compounds in the blood, reaches very low levels (about 1%), 6–10 min after the injection. Our results are consistent with Andersen's data. Moreover, we suggest that perhaps octanol also extracts a fraction of NDR, which is probably still lipophilic but is not available for extraction across the BBB (HMPAO bound to lipoproteins and chylomicra) (4). If this is so, NDR_E can be

TABLE 2
Mean rCBF and rCl_{pao} Values

Region	ROIs volume (cm ³)	rCBF (ml/min/g)	rCl _{pao} (ml/min/g)
AS frontal	6.97 \pm 0.25	0.743 \pm 0.030	0.399 \pm 0.018
PS parietal	9.63 \pm 0.15	0.721 \pm 0.017	0.406 \pm 0.018
Cingulum	7.60 \pm 0.35	0.902 \pm 0.017	0.473 \pm 0.021
Prefrontal	6.40 \pm 0.26	0.730 \pm 0.021	0.392 \pm 0.023
Temporal	6.77 \pm 0.22	0.716 \pm 0.022	0.393 \pm 0.020
Occipital	3.99 \pm 0.26	0.778 \pm 0.023	0.403 \pm 0.022
Thalamus	2.88 \pm 0.18	0.811 \pm 0.024	0.431 \pm 0.026
Basal ganglia	3.62 \pm 0.12	0.692 \pm 0.029	0.415 \pm 0.024
Gen. semiovale	4.50 \pm 0.20	0.486 \pm 0.026	0.282 \pm 0.019
Frontal white	1.21 \pm 0.08	0.418 \pm 0.017	0.248 \pm 0.016
Grey/White ratio		1.69 \pm 0.05	1.57 \pm 0.04

Values are expressed as mean \pm s.e.m.

AS = anterosuperior and PS = posterosuperior.

considered a "false signal" for the octanol extraction technique.

Our assumption as regards the constancy of K ($NDR_E/NOER$) during the arterial sampling is important. A chromatographic analysis (paper or liquid chromatography) that separates NDR_E from DR could further support this assumption. However, it is worth noting that the weight of the correction based on the K value that we propose is not linear in time, since it is proportional to $NOER$. Indeed, the correction weight is minimal in the first part of the arterial sampling, when the final arterial input value is largely determined. Instead, the correction effect becomes significant near the end of the sampling (Fig. 2), when the constancy of K is demonstrated by the plateau in the course of the $OER/NOER$ curve (Fig. 1).

The choice of microspheres as a reference tracer is favourable from a technical point of view, since the same radioactive label (^{99m}Tc) and the same instrumentation are used. Unfortunately, the microsphere method, although it is well-documented in experimental animals (14) and in human subjects (15), is not widely used because of the difficulty associated with the route of administration.

Our results show cortical $rCBF$ values which are higher than those reported in the study in humans with microspheres and PET (15). Indeed, Brooks et al. (15) sampled brain activity with circular ROIs measuring 2 cm in diameter. For such ROIs, their FWHM (17 mm) gives a "relative ECT value" of 0.65 (16). Therefore, according to Brooks et al., their cortical samples are approximately 50% white and 50% grey matter. Our SPECT FWHM (8 mm) would yield a "relative ECT value" close to 1 for the same sized ROIs. Therefore, it is more likely that our anatomical cortical ROIs measure the activity content of the cortex alone.

Moreover, considering that the brain is composed of about 62% white matter and 38% grey matter (17), our average $rCBF$ values for grey and white matter (0.74 and 0.45 ml/min/g, respectively) yield a total brain blood flow of 0.56 ml/min/g. This is in accordance with the values reported by Lassen for the entire brain (18).

Microsphere images show a higher contrast than the HMPAO ones. This result is consistent with the extraction limitations and back-flux of HMPAO while the microspheres are trapped and retained.

For these same kinetic differences, rCl_{pao} values are systematically lower than $rCBF$ values. Since both extraction limitation and back-diffusion are flow-dependent mechanisms, a non-linear relationship should be expected between the two measures. This result would also be expected from the various contrasts of microsphere and HMPAO SPECT images. The high significance of linear regression between $rCBF$ and rCl_{pao} is probably related to the limited range of the perfusion values of our series (0.28–0.96 ml/min/g). The linear regression is therefore valid only in this range. Furthermore, the linear regression that we obtained is also consistent with the various con-

trasts of microsphere and HMPAO SPECT images, because the regression intercept is above zero (0.07 ml/min/g).

In this limited range, the regression parameters can be used in a "data model" to obtain perfusion values from rCl_{pao} values. Assuming that the parameters regulating the brain kinetics of HMPAO can be considered stable with time in the same subject and between different subjects, rCl_{pao} itself—because of the high significance of the regression with $rCBF$ —can be used directly as a perfusion index for clinical use.

With regard to the HMPAO retained fraction in the ROIs studied, we found a value of 0.55 ± 0.10 (mean \pm s.d.). Lassen et al. (2) report a mean retained fraction of 0.38 ± 0.06 ($E \cdot R'$) for the entire brain in neurologic patients. The difference between these two results may, in part, be attributed to the following: the different type of subjects studied, the small sample size of both series and the different cerebral volumes sampled (entire brain versus brain regions). Moreover, the two studies are methodologically different and in our procedure the correction for attenuation and scatter is far from being a deterministic one.

We believe that rCl_{pao} is the best approximation of $rCBF$ values that can be provided by slowly rotating gamma camera SPECT devices. Indeed, when our data model is applied, the rCl_{pao} data can be converted into $rCBF$.

We suggest introducing our method to evaluate the diffusible input in a more complete modelistic approach such as that proposed by Matsuda et al. (6). This would help reduce the number of fitted parameters by eliminating the blood conversion rate constant.

In conclusion, a strong correlation exists between brain perfusion and the SPECT measurement of rCl_{pao} with the method presented in this work. The study of a wider subject population with both microspheres and HMPAO may be useful to assess the use of data models such as the linear regression that we used. However, it must be remembered that the clinical application of this method may prove quite critical in the transfer of the data model approach from controls to patients.

ACKNOWLEDGMENTS

The authors wish to thank Prof. Gianni Bisi, Prof. Giuseppe La Cava, and Dr. Antonio Castagnoli for valuable discussions, Mr. Giannetto Comis for the development of the PC image representation software and Dr. Elizabeth Guerin for her assistance in preparing the manuscript. They are also grateful to the technicians of the Nuclear Medicine Unit for their collaboration and thank Amersham Italy (Amity) for its financial support.

This work was partially supported by MURST-60% grants.

REFERENCES

1. Neirinckx RD, Canning LR, Piper IM, et al. [^{99m}Tc]d,l-HM-PAO: a new radiopharmaceutical for SPECT imaging of regional cerebral blood perfusion. *J Nucl Med* 1987;28:191–202.
2. Lassen NA, Andersen AR, Friberg L, Paulson OB. The retention of [^{99m}Tc]

- d,1-HM-PAO in the human brain after intracarotid bolus injection: a kinetic analysis. *J Cereb Blood Flow Metab* 1988;8:S13-S22.
3. Lear JL. Initial cerebral HM-PAO distribution compared to LCBF: use of a model which considers cerebral HM-PAO trapping kinetics. *J Cereb Blood Flow Metab* 1988;8:S31-S37.
 4. Andersen AR, Friberg H, Lassen NA, Kristensen K, Neirinckx RD. Assessment of the arterial input curve for [^{99m}Tc]-d,1-HM-PAO by rapid octanol extraction. *J Cereb Blood Flow Metab* 1988;8:S23-S30.
 5. Kuhl DE, Barrio JR, Huang S, et al. Quantifying local cerebral blood flow by N-isopropyl-p-[¹²⁵I]iodoamphetamine (IMP) tomography. *J Nucl Med* 1982;23:196-203.
 6. Matsuda H, Oba H, Seki H, et al. Determination of flow and rate constants in a kinetic model of [^{99m}Tc]-hexamethyl-propylene amine oxime in the human brain. *J Cereb Blood Flow Metab* 1988;8:S61-S68.
 7. Bacciotini L, Lunghi F, Pupi A, et al. Evaluation of technetium-99m-cyclobutylpropylene amine oxime as a potential brain perfusion imaging agent for SPECT. *Eur J Nucl Med* 1990;17:242-247.
 8. Lentner CS. *Dat fisico-chimici*. In: Lentner CS, ed. *Tavole scientifiche Geigy*, 8th ed. Vicenza: C'ibou-Geigy Edizioni; 1985: (III):67-71.
 9. Formiconi AR, Pupi A, Passeri A. Compensation of spatial system response in SPECT with conjugate gradient reconstruction technique. *Phys Med Biol* 1989;34:69-84.
 10. Formiconi AR. Oblique angle sections in emission computed tomography. *J Nucl Med All Sci* 1984;28:109-114.
 11. De Cristofaro MTR, Mascalchi M, Pupi A, Nencini P, et al. Subcortical arteriosclerotic encephalopathy: single-photon emission computed tomography-magnetic resonance imaging correlation. *Am J Physiol Imaging* 1990;5:68-74.
 12. Formiconi AR, Pupi A, De Cristofaro MTR, Dal Pozzo G, Fagnoli R, Meldolesi U. Superimposition of brain sections from different acquisition techniques (CT and SPECT). *J Cereb Blood Flow Metab* 1989;9:S413.
 13. Pupi A, De Cristofaro MTR, Formiconi AR, et al. A brain phantom for studying contrast recovery in emission computerized tomography. *Eur J Nucl Med* 1990;17:15-20.
 14. von Ritter C, Hinder RA, Womack W, et al. Microsphere estimates of blood flow: methodological considerations. *Am J Physiol* 1988;254:G275-G279.
 15. Brooks DJ, Frackowiack RS, Lammertsma AA, et al. A comparison between regional cerebral blood flow measurements obtained in human subjects using ¹¹C-methylalbumin microsphere, the C¹⁵O₂ steady-state method, and positron emission tomography. *Acta Neurol Scand* 1986;73:415-422.
 16. Kojima A, Matsumoto M, Takahashi M, Hirota Y, Yoshida H. Effect of spatial resolution on SPECT quantification values. *J Nucl Med* 1989;30:508-514.
 17. Chiarugi G. Generalita' sull' encefalo. In: *Istituzioni di anatomia dell' uomo*, ninth edition. Milano: Casa Editrice Francesco Vallardi; 1965:75-88.
 18. Lassen NA. Normal average value of cerebral blood flow in younger adults is 50 ml/100 g/min. *J Cereb Blood Flow Metab* 1985;5:347-349.

EDITORIAL

Toward Absolute Quantitation of Cerebral Blood Flow Using Technetium-99m-HMPAO and a Single Scan

A simple method for estimating absolute regional cerebral blood flow (rCBF) using a ^{99m}Tc radiopharmaceutical would be useful for research and clinical applications. In our own clinical studies using ^{99m}Tc-HMPAO, we often ponder whether the activity in the right hemisphere is down or the left hemisphere up and whether blood flow is globally changed. It would be helpful to have ready answers to such questions, and the work of Pupi et al. is a welcome step in that direction.

Techniques to quantitate rCBF using kinetic analysis of ^{99m}Tc-HMPAO uptake require fixed-ring cameras that are sufficiently sensitive to sample regional brain activity on a minute by minute basis. Kinetic approaches also require a lengthy and sophisticated analysis, and in general, the estimation of rate constants can be biased significantly by relatively

small systematic errors in data acquisition. Thus, a kinetic analysis of HMPAO uptake, while theoretically sound and very much appropriate for research, is not at all suited to routine clinical use.

In contrast, the technique described by Pupi et al. requires only one SPECT measurement of regional brain activity, performed at a time after injection when the amount of radiopharmaceutical in the brain is essentially stable. This single-scan approach makes it possible, in theory, to quantitate rCBF using any SPECT system. Since the amount of brain activity depends not only on flow but also on the amount of radiopharmaceutical delivered to the brain, the single-scan technique still requires substantial laboratory work: after rapid arterial blood sampling, the portion of ^{99m}Tc-HMPAO that is freely diffusible across the blood brain barrier must be distinguished from total blood activity through a rapid octanol extraction technique. The resulting arterial input function is summarized by its integral, which, along with the

single SPECT measurement of brain activity, is used to compute a regional brain clearance of HMPAO.

The authors compare the regional clearance of HMPAO with rCBF measured through the injection of microspheres into the left ventricle during angiography. The microsphere technique is theoretically sound and serves as an excellent standard against which quantitation using HMPAO can be validated. One drawback of the experimental design is that the HMPAO and microsphere studies were performed on different days, apparently without controlling factors which may affect rCBF, such as changes in sensory stimulation and ventilation.

While the single scan approach would significantly simplify and therefore extend the ability to measure cerebral blood flow, the technique in its present form may not yet be ready for routine use. One concern is that, after placement of an arterial line, the performance of rapid blood sampling and octanol extraction is at least moderately labor-intensive. Before switch-

Received Apr. 4, 1991; accepted Apr. 4, 1991.
For reprints contact: Zachary Rattner, MD, Assistant Professor, Department of Diagnostic Radiology, Yale University of Medicine, 333 Cedar St., P.O. Box 333, New Haven, CT 06510